

# Cantilever-enhanced photoacoustic spectroscopy applied in the research of natural and synthetic calcium phosphate

A Brangule<sup>1,2</sup>, K A Gross<sup>2</sup>, V Stepanova<sup>3</sup>

<sup>1</sup>Dept.of Human Physiology and Biochemistry, Riga Stradiņš University, Dzirciema 16, LV-1007, Riga, Latvia

<sup>2</sup>Biomaterials Research Laboratory, Riga Technical University, P.Valdena 3, LV-1048, Riga, Latvia

<sup>3</sup>Institute of General Chemical Engineering, Riga Technical University, P.Valdena 3, LV-1048, Riga, Latvia

E-mail: agnese.brangule@rsu.lv

**Abstract.** This study demonstrates the significant potential of cantilever-enhanced Fourier transform infrared photoacoustic spectroscopy (FTIR PAS) principles. The improved sensitivity and reproducibility of this method presents a potent tool in the study of biomaterials. The article discusses aspects of the application of cantilever-enhanced FTIR PAS in the research of natural and biological calcium phosphate and the statistical evaluation of the FTIR PAS sampling method. The improved constructions of the FTIR PAS accessory reduce limitations of the conventional capacitive microphone and provide a sensitive tool for samples or processes unreachable by more traditional transmittance methods, or ATR sampling technique. The most common and important applications have been discussed in-depth to show the wide range of problems solved by FTIR PAS.

## 1. Introduction

This article discusses the aspects of the validation of the Fourier transform infrared cantilever-enhanced photoacoustic spectroscopy's method and its application in the characterization of natural and synthetic calcium phosphate. Nanosized carbonated calcium phosphate (amorphous and crystalline) play an important role in the formation of natural and synthetic biomaterials [1]. Various techniques, such as x-ray diffraction (XRD) and spectroscopic methods (IR and Raman) can be applied in the characterization of calcium phosphates [2-4]. In previous studies, the FTIR spectroscopy's method (especially the transition mode) was the most widely used method because it can display characteristic absorption peaks over a large range of crystallinity [2,5]. The main problem with samples, when using FTIR in the characterization of calcium phosphates, is that almost all solid materials are too opaque for the direct transmission mode. This problem can be solved by reducing the optical density of samples by mixing or pressing the powder with KBr, or using various sampling techniques [6,7].

This article discusses the aspects of the cantilever-enhanced FTIR PAS application in the research of natural and biological calcium phosphate. The major advantage of the photoacoustic effect is the fact that sensitivity is not dependent on the optical path length. This allows high sensitivity from short absorption path length, and a highly linear concentration response over a wide dynamic measurement range, from very low sample volumes [8,9]. In previous works in the characterization of calcium



phosphates the sensor used was a pressure sensor, the condenser microphone, which mainly limits the sensitivity of the photoacoustic detection [10]. Our study is based on PAS with an interferometer cantilever detector that allows for increased sensitivity, even several orders of magnitude higher than the condenser microphone. Due to the high detector sensitivity, PAS can work on a small scale, previously reached only by IR microscopy. In the scale of photoacoustic spectroscopy, the samples are considered remarkably small, and are hence called micro samples [11]. Previous studies reported that PAS with a cantilever detector is a valuable tool for studying samples of various morphologies due to the ease of sample preparation and depth profiling capabilities [9]. This study is divided into two parts: a validation of the FTIR PAS method and a comparison with FTIR transmission and applications, focusing on the advantages of PAS and the limitations of FTIR transmission.

## 2. Materials and Methods

### 2.1. Characterization Methods

**2.1.1. PAS-FTIR spectroscopy (FTIR PAS).** PAS spectra were taken at  $450 - 4000 \text{ cm}^{-1}$  at a resolution of  $4 \text{ cm}^{-1}$ , and the average was made from 10 scans with Gasera PA301, with the cell being filled with helium gas (flow  $0.5 \text{ l/min}$ ). A special preparation method was not required for the synthesized powders and bone powders;  $0.01 \text{ g}$  of powder was placed in the PAS cell. The pressed calcium phosphate pellet was placed in the PAS cell as well.

**2.1.2. FTIR Transmission (FTIR KBr).** Transmission spectra were taken at  $450 - 4000 \text{ cm}^{-1}$  at a resolution of  $4 \text{ cm}^{-1}$ , and the average was made from 16 scans with the Perkin Elmer Spectrum Two. Synthesized powders were pressed into KBr pellets.

**2.1.3. X-ray powder diffraction (XRD).** Diffraction patterns were recorded entirely for the powders used in the validation process with the Bruker D8 ADVANCE diffractometer, from  $5^\circ$  to  $60^\circ$  using Cu  $K\alpha$  radiation ( $\lambda = 1.54 \text{ \AA}$  generated at  $40 \text{ mA}$  and  $40 \text{ kV}$ ) at a step size of  $0.2^\circ$ . The crystallinity and crystallite size was evaluated using Profex 3.7.0 software [12].

**2.1.4. Analysis of spectra.** The FTIR spectra were viewed and smoothed with the freeware software *Specwin32*, *SpectraGryph 1.0* and *Grams/AI*. The baseline correction and curve-fitting analysis were performed using the software *MagicPlotStudent*. Deconvolution and convolution involved both Lorentzian and Gaussian curve fitting. Statistical analyses, such as the Pearson Product-Moment Correlation Coefficient (PPMCC), Cluster Analysis (CA) Chebyshev Distance Matrix and the Principal Component Analysis (PCA) were performed using software *Statistica 10.0*.

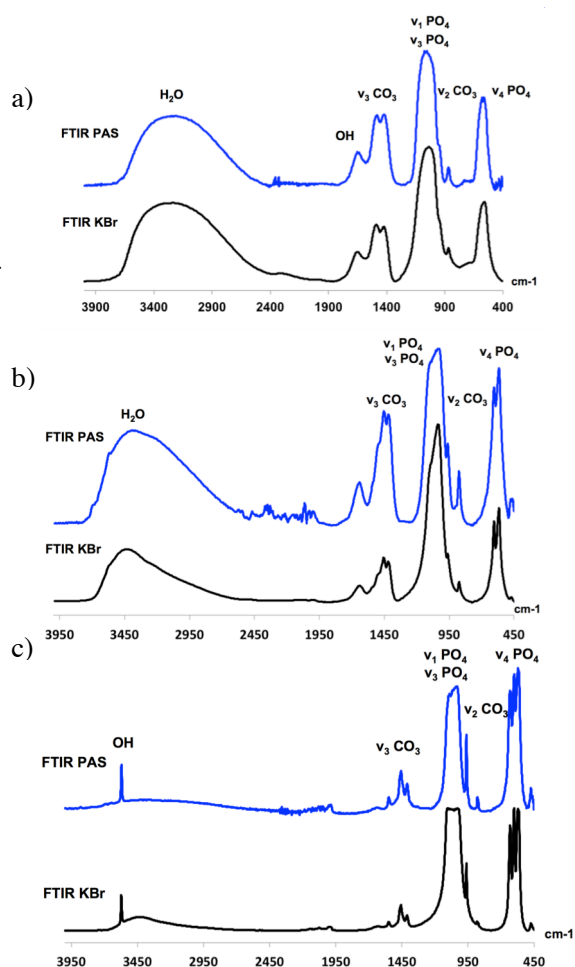


Figure 1. FTIR PAS and FTIR KBr (spectra: a) v-1 amorphous; b) v-2 poorly crystalline c) v-3 crystalline CCP powder.

## 2.2. Materials

**2.2.1. Synthesis.** Carbonate containing calcium phosphate (CCP) powders were obtained using following reactants: a solution containing  $\text{Ca}(\text{NO}_3)_2$  and 30% ammonia mixed with a solution containing  $(\text{NH}_4)_2\text{HPO}_4$  and  $(\text{NH}_4)_2\text{CO}_3$  at room temperature, filtered and washed several times with deionized water containing ammonia.

**2.2.2. Powders for the validation process.** To adjust the particle size and composition of powders, drying was conducted in a freeze-drier at  $-50\text{ }^\circ\text{C}$  for 72 h or in a convection oven at  $200\text{ }^\circ\text{C}$ . A part of the freeze-dried powder was heated at  $900\text{ }^\circ\text{C}$ . The powders were labelled as v-1, v-2, v-3 according to the particle size, where v-1 represents the amorphous powder (particle size  $<1\text{ nm}$ ), v-2 depicts a poorly crystalline (particle size 20 nm), but v-3 is a crystalline powder (particle size 70 nm).

## 3. Results and Discussions

### 3.1. Validation of FTIR PAS.

In order to validate the usage of PAS spectroscopy in the field of calcium phosphate, PAS spectra were recorded for the three most typical nanosized CCP powders: amorphous (v-1), poorly crystalline (v-2), and crystalline (v-3). To evaluate this method, FTIR PAS spectra were compared with the transmission FTIR spectra for the same CCP powders. The CCP samples of both FTIR sampling methods were examined in the wavenumber range  $400 - 4000\text{ cm}^{-1}$  (Fig. 1). A comparison of FTIR PAS and FTIR KBr methods by qualitative features showed at well-defined peaks:  $460 - 700\text{ cm}^{-1}$  ( $\nu_4\text{ PO}_4$ ,  $\nu_L\text{ OH}$ ),  $900 - 1200\text{ cm}^{-1}$  ( $\nu_1$ ,  $\nu_3\text{ PO}_4$ ) and  $1340 - 1800\text{ cm}^{-1}$  ( $\nu_3\text{ CO}_3^{2-}$  non-apatitic, type A and B) for both methods and all three powders; the presence of OH bands at  $3750\text{ cm}^{-1}$  for both methods in the crystalline powder (v-3) and the presence of  $\text{H}_2\text{O}$  at  $2500 - 3900\text{ cm}^{-1}$  for amorphous powders (v-1 and v-2). FTIR PAS method is more sensitive to  $\nu_2\text{ CO}_3^{2-}$  group detection in the  $860 - 890\text{ cm}^{-1}$  region. PAS spectra were noisy in  $1950 - 2450\text{ cm}^{-1}$  region, but they have no effect on CCP characteristic groups in  $\nu_2$ ,  $\nu_3\text{ CO}_3^{2-}$ ,  $\nu_4\text{ PO}_4^{3-}$ ,  $\nu_L\text{ OH}/\text{H}_2\text{O}$  band region. A chemometric analysis of FTIR spectra was conducted in the region with an analytical significance of  $400 - 1800\text{ cm}^{-1}$ . Characterizations with PPMC coefficients were performed at the  $460 - 700\text{ cm}^{-1}$  ( $\nu_4\text{ PO}_4$ ,  $\nu_L\text{ OH}$ ) and  $1340 - 1800\text{ cm}^{-1}$  ( $\nu_3\text{ CO}_3^{2-}$  non-apatitic, type A and B) region. The calculated PPMC coefficients in the defined spectral regions show a strong comparability of methods (Table 1). A cross-validation with PPMCC was performed between amorphous (v-1) and crystalline (v-3) powders recorded by PAS and FTIR KBr mode (Table 1). In the cross-validation process, PPMCC shows a differentiation between amorphous and crystalline

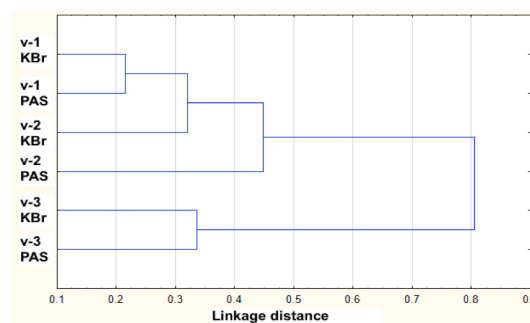


Figure 2. Hierarchical cluster method (Chebyshev Distance Matrix) for FTIR PAS and FTIR KBr and amorphous, poorly crystalline and crystalline powders in  $400 - 1800\text{ cm}^{-1}$  region.

**Table 1.** PPMCC of PAS FTIR vs FTIR KBr spectra

| Spectra region   | 460 – 700 $\text{cm}^{-1}$<br>( $\nu_4\text{ PO}_4$ ,<br>$\nu_L\text{ OH}$ ) | 1340–1800 $\text{cm}^{-1}$<br>( $\nu_3\text{ CO}_3^{2-}$<br>non-apatitic,<br>type A and B) |       |
|------------------|--|--|-------|
| Validation       | v-1<br>Amorphous   | 0.991  | 0.970 |
|                  | v-2<br>Poorly<br>crystalline   | 0.963  | 0.969 |
|                  | v-3<br>Crystalline   | 0.979  | 0.986 |
| Cross-validation | PAS (v-1;<br>amorphous) vs<br>FTIR KBr (v-<br>3; crystalline)                | 0.730  | 0.867 |
|                  | PAS (v-3;<br>crystalline) vs<br>FTIR KBr<br>(v-1;<br>amorphous)              | 0.712  | 0.817 |

powder. The Chebyshev Distance Matrix (Figure 2) confirms that both methods show a significant difference between amorphous and crystalline CCP powder, and can be used in their characterization.

The validation method, being a very important step in PAS, was applied for the process characterization. In our research PAS spectra were recorded for amorphous ( $v_1$ ) powder, which was heated at different temperatures for a constant period of time. Characteristic bands were assigned to literature data [2,13]. Spectra obtained in the  $460 - 700 \text{ cm}^{-1}$  ( $v_4 \text{ PO}_4$ ,  $v_L \text{ OH}$ ),  $1340 - 1600 \text{ cm}^{-1}$  ( $v_3 \text{ CO}_3^{2-}$  nonapatitic, type A and B) and  $3500 \text{ cm}^{-1} - 3700 \text{ cm}^{-1}$  (OH) region show a considerable change in peak shape and position (Fig. 3). Additional information on CCP powders can be obtained from all three regions: structure, composition, and level of crystallinity. By splitting  $v_4 \text{ PO}_4$  peaks into a well-defined doublet, the rising of the third band  $630 \text{ cm}^{-1}$ , the rising of OH  $3750 \text{ cm}^{-1}$  bands, and changes of to the A-type and B-type carbonates can be interpreted as higher crystallinity and a transformation to hydroxyapatite structure. The results of the study obtained by FTIR PAS confirmed the usage of this method in the characterization of the process.

### 3.2. Application of FTIR PAS.

Three methods are presented, each one typical for a particular area of application, or of an important consideration in FT-IR PAS measurements. The methods were the following:

1. Process characterization on the surface.
2. Characterization of wet powders.
3. Characterization of microsamples.

#### 3.2.1. Process characterization on the biomaterial surface during the bacteria colonization process.

Microbial analysis was chosen as a model by which we wanted to observe two processes simultaneously: a presence of functional groups of pressed amorphous CCP pellet and a presence of bacteria on its surface. Samples were prepared according to the method described in previous

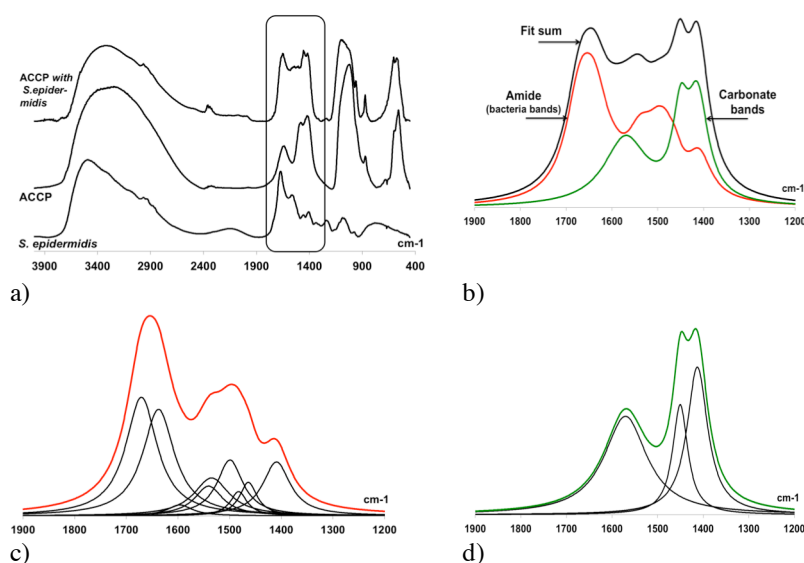


Figure 4. a) FTIR PAS spectra of bacteria *S. epidermidis*, CCP and CCP surface and bacteria; b) The Deconvolution of ACCP surface with *S. epidermidis* showing deconvoluted and convoluted c) Amide band and d) Carbonate band.

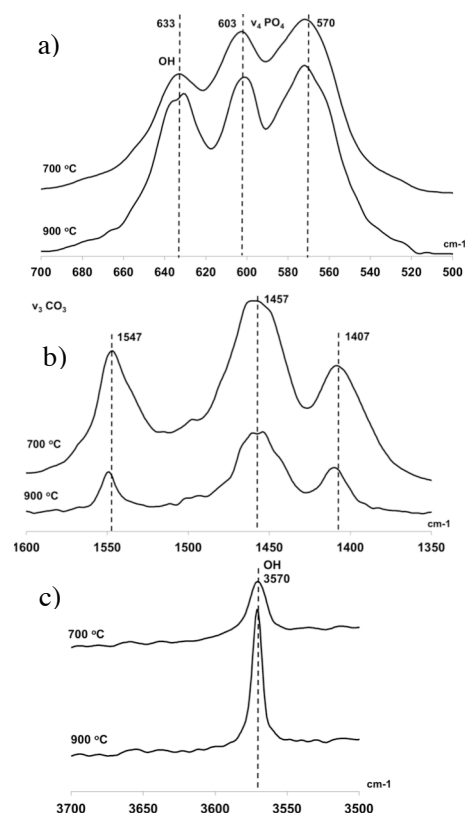


Figure 3. Effect on heating temperature on  $v_1$  amorphous CCP powder (in the PAS spectra region: a)  $460 - 700 \text{ cm}^{-1}$ ; b)  $1340 - 1600 \text{ cm}^{-1}$ ; c)  $3500 \text{ cm}^{-1} - 3700 \text{ cm}^{-1}$ ).

studies [14,15]. Spectra were obtained on the surface of the pressed CCP pellet before and after the colonization of the *S.epidermidis* bacteria and of the separately grown bacteria (Fig. 4a). The novelty of the application of the sensitive cantilever enhanced FTIR PAS method is the opportunity to simultaneously identify carbonate bands ( $1400\text{--}1540\text{ cm}^{-1}$ ;  $\nu_3\text{CO}_3$  A, B), OH bands ( $1640\text{ cm}^{-1}$ ) from CCP

Table 2. Advantages and disadvantages of cantilever PAS-FTIR

| Advantages  | Disadvantages   |
|---|---|
| <ul style="list-style-type: none"> <li>• Direct surface measurement;</li> <li>• No effect of peak over saturation;</li> <li>• Very high reproducibility;</li> <li>• No risk of sample contamination;</li> <li>• Measure possibility of measurement of samples with high humidity;</li> <li>• Research possibility of research of reaction transformation, crystallization by direct measurement.</li> </ul> | <ul style="list-style-type: none"> <li>• Additional cost of unite;</li> <li>• Limited size of samples (<math>D \sim 1\text{ cm}</math>);</li> <li>• Higher spectral noise.</li> </ul> |

surface, and amide I, II, III bands which suggested the presence of *S.epidermidis* bacteria [14,16,17]. The determination of characteristic bands is limited by overlapping amide, carbonate and OH bands in the  $1200\text{--}1900\text{ cm}^{-1}$  region (Fig. 4b). The only deconvolution of spectra shows detailed information about inorganic ( $\text{CO}_3$ , OH from CCP) and organic (amides in bacteria) matter (Fig. 4c; 4d).

**3.2.2. Characterization of wet powder.** A spray-drying method was chosen to obtain amorphous CCP powders with a constant moisture content (9%). A wet sample analysis allows for time saving that is spent on drying (2h) and to evaluate faster the next steps in the powder processing more quickly. Other FTIR sampling methods (transmission, KBr) can't be used due to the drying effect of KBr and the fast drying and crystallization of a sample on the DRIFT sampling stick. During this experiment, FTIR PAS spectra were recorded for wet CCP with and without contamination with nitrate and ammonia ions (Fig. 5), because contamination with nitrate and ammonia ions can proceed if synthesized samples are not properly washed with distilled water after synthesis. The obtained PAS spectra show characteristic CCP bands in both poor and contaminated powder. In contaminated powder, the peaks near  $3000\text{--}3500\text{ cm}^{-1}$ ,  $2500\text{ cm}^{-1}$ ,  $1000\text{--}1500\text{ cm}^{-1}$  suggest the presence of nitrate and ammonia ions. FTIR PAS is sensitive to nitrates and spectra can be recorded for wet CCP powders.

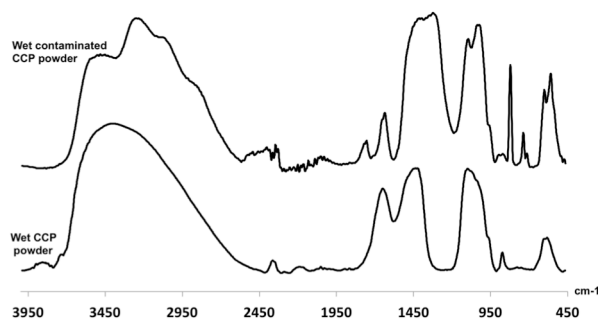


Figure 5. FTIR PAS of wet poor and wet contaminated CCP.

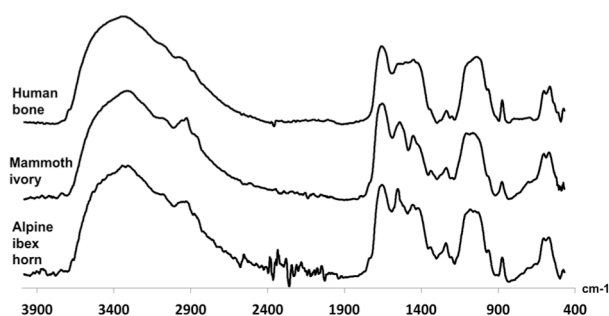


Figure 6. FTIR PAS spectra of biological samples: human bone, mammoth ivory, and Alpine ibex horn.



*3.2.3. Characterization of microsamples.* Artefacts and organic gem materials are stored in various collections or museums. Researchers should be very accurate during the process of studying and analysing them while being as non-destructive as possible. At the same time, they should be able to answer questions concerning their identification, particularly – what is this object made of; postulate provenance, and authenticity [18]. In the last method, we wanted to represent cantilever enhanced FTIR PAS as a sensitive, representative, and non-destructive tool with minimum sample preparation. The recorded spectra of archaeological human bone and organic gem material showed well-defined peaks:  $460 - 700 \text{ cm}^{-1}$  ( $\nu_4 \text{ PO}_4$ ,  $\nu_L \text{ OH}$ ),  $900 - 1200 \text{ cm}^{-1}$  ( $\nu_1$ ,  $\nu_3 \text{ PO}_4$ ) and the presence of  $\text{H}_2\text{O}$  at  $2500 - 3900 \text{ cm}^{-1}$ . The  $1000 - 1900 \text{ cm}^{-1}$  region has an overlap of amide and  $\text{CH}_2$  peaks (from organic matter), with carbonate peaks (from inorganic matter), which can be distinguished only by deconvolution [19].

#### 4. Conclusions

This comparative study shows significant potential for cantilever-enhanced photoacoustic spectroscopy. The improved sensitivity and reproducibility of the method, gives a potent tool for the study of reaction kinetics and the transformation of compound phases. The non-destructive nature of the method provides advantages for the study of samples, where the need to conserve material or study of fixed points exists. At the same time, the method has significant limitations. Notably, sample size limitation, reduced signal/noise, and the additional cost of the sampling device. A photoacoustic sampling device gives valuable information for complicated samples, which are unreachable for ATR, DRIFT or transmittance sampling equipment.

#### References

- [1] Legeros R Z 1994 In Brown P W, Constantz B (Eds.), *Hydroxyapatite and Related Materials*, Boca Raton, CRC Press, pp 3-28.
- [2] Eichert D *et al* 2007 In Kendall JB (ed) *Biomaterials research advances*. Nova Science, New York, pp 93-145.
- [3] Gadaleta S J *et al* 1996 *Calcif Tissue Int* **58** 9–16.
- [4] Ślósarczyk A *et al* 2005 *J. Mol. Struct.* **744–747** 657–61.
- [5] Rey C *et al* 1991 *Calcif Tissue Int* **49** 251.
- [6] Rockley M G *et al* 1980 *Spectrosc.* **34** 405-406.
- [7] Colthup N B *et al* 1990 *Introduction to infrared and Raman spectroscopy*, 3<sup>rd</sup> Edn, Academic Press.
- [8] McClelland J F *et al* 2006 *Photoacoustic Spectroscopy*. In *Handbook of Vibrational Spectroscopy*.
- [9] Uotila J *et al* 2008 *Appl. Spectrosc.* **62** 655-660.
- [10] Rehman I *et al* 1997 *J. Mater. Sci.* **8** 1-4.
- [11] Lehtinen J *et al* 2013 *Appl. Spectrosc.* **67**, 846–850.
- [12] Döbelin N *et al* 2015 *J. Appl. Crystallogr.* **48**, 1573-1580.
- [13] Fleet M E *et al* 2004 *Am. Mineral.* **89** 1422-1432.
- [14] Brangule A *et al* 2016 *Key Eng. Mater.* **720** 125-129
- [15] Slobbe L *et al* 2009 *J. Clinical Microbiol.* **47** 885–888.
- [16] Káflak A *et al* 2011 *J. Molec. Struct.* **997** 7-14.
- [17] Ardeleanu M *et al* 1992 in: *Springer Series in Optical Sciences* **69**, Springer-Verlag Berlin, Heidelberg pp 81-84.
- [18] Gu C *et al* 2013 *Spectrochim. Acta. A. Mol. Biomol. Spectrosc.* **103** 25–37.
- [19] Brangule A *et al* 2015 *IOP Conf. Series: Mater. Sci. Eng.* **77**.